# Shear-Induced Orientations and Textures of Nematic Wormlike Micelles

**Denis C. Roux, Jean-François Berret,* and Grégoire Porte**

*Groupe de Dynamique des Phases Condensees, URA CNRS 233, Université de Montpellier II, F-34095 Montpellier Cedex 05, France*

**Edith Peuvrel-Disdier**

*Centre de Mise en Forme des Matériaux, Ecole des Mines de Paris, URA CNRS 1374, BP 207, F-06904 Sophia Antipolis, France*

**Peter Lindner**

*Institut Laue-Langevin, BP 156, F-38042 Grenoble Cedex 9, France*

*Received July 20, 1994; Revised Manuscript Received November 10, 1994*[⊗]

ABSTRACT: We have used rheology, rheo-optical observations, and small-angle neutron scattering under shear to investigate the flow, orientation, and texture properties of nematic solutions of equilibrium or "living" polymers. The elementary objects of these liquid crystalline phases are wormlike micelles, that is, flexible cylindrical aggregates made of amphiphile molecules. The aqueous surfactant solutions investigated here (cetylpyridinium chloride and hexanol in 0.2 M NaCl-brine) exhibit the classical structural sequence: isotropic/nematic/hexagonal with increasing surfactant concentration $\phi$. The nematic phase observed for $\phi$ = 34%−38% consists of very long cylindrical micelles closely packed parallel to each other, thus producing long-range orientational order. We have shown that when subjected to a steady shear, the nematic phase of living polymers behaves very similarly to that of the conventional liquid crystalline polymers. From the rheo-optical observations, we demonstrated that so-called band textures show up perpendicular to the flow direction after cessation of the shearing, indicating a modulation of the director orientation. As for liquid crystalline polymers, these textures are interpreted in terms of relaxation of the Frank distorsional energy accumulated during the flow. The time evolution of the average band spacing of the texture could be determined and compared to recent theoretical predictions; e.g. in the low-shear regime the squared band spacing scales linearly with time. We also study the evolution of the order parameter of the nematic state (actually spatially averaged over the mesoscopic textures observed during the flow or at rest) determined from small-angle neutron scattering spectra obtained under shear. As remarkable features, we found out that above a characteristic shear rate, $\dot{\gamma}_c$, the nematic living polymers form an orientational monodomain which in addition is remarkably stable over a long period of time. The present data are compared to those reported for liquid crystalline polymers.

## I. Introduction

It is now well established that under appropriate conditions, the amphiphilic molecules spontaneously self-assemble to form highly flexible locally cylindrical aggregates with an average size approaching several microns.[1] The typical radii of these wormlike micelles are about 20−25 Å, and the persistence length, which is related to the flexibility of the polymer-like chain has been estimated to be ~150−200 Å. As far as the static and quasi-static properties are concerned, it has been shown that semidilute solutions of wormlike micelles resemble strongly those of conventional polymers.[2] However, unlike ordinary polymers, the micellar chains are *equilibrium* objects: they can reversibly break and recombine. At the origin of the terminology usually employed for these systems, namely equilibrium or "living" polymers, this property has crucial consequences on their flow behaviors.

The linear and nonlinear viscoelastic responses of the isotropic solutions of living polymers have been extensively studied over the past few years, both theoretically[3] and experimentally.[4−8] The semidilute ($\phi \approx$ 1−10%, where $\phi$ is the total surfactant concentration) and concentrated ($\phi \leq$ 30%) regimes were investigated, and a successful picture of the microscopic mechanisms able to relax external applied stresses has been developed. The linear rheology appears to be dominated by reptation and by reversible breaking and recombinations of the chains. At still higher concentration, $\phi >$ 40%, the micellar threads orient at a large scale due to steric constraints, resulting in an ordered phase of hexagonal symmetry. But, more interestingly, a nematic calamitic ($N_c$) phase[9−11] is sometimes observed at intermediate concentrations between the isotropic ($L_1$) and the hexagonal (H) phases (typically for 30% < $\phi$ < 40%). Concerning the structure, scattering experiments[10] have revealed that the nematic phase indeed consists of very long cylindrical micelles closely packed parallel to each other, thus producing long-range orientational order. Up to now, however, little attention has been paid to the rheological properties of such nematic phases made of wormlike micelles as well as to the possible molecular alignment induced by a shearing field.

On the other hand, the rheology of liquid-crystalline polymers (LCP) has been a research field of intense activity during the past decade. The most thoroughly studied LCP's are the systems with polypeptidic or cellulose chains (e.g. PBLG[12−14] and HPC,[15] respectively). For these systems, in absence of flow, it is now admitted that the orientational correlations related to the long-range nematic order result in a polydomain structure whose most obvious property is the nonho-

[⊗] Abstract published in *Advance ACS Abstracts,* January 15, 1995.

0024-9297/95/2228-1681$09.00/0 

mogeneous birefringence of light. Each domain is then characterized by a homogeneous average molecular orientation, defining for nematics the director axis. Such a polydomain spatial arrangement is comparable to what is known in solid state physics as polycrystalline materials, as long as the translational degrees of freedom are replaced by orientational ones.

A great amount of experimental data using, e.g., the optical microscopy under shear has shown the existence of so-called **textures** during and after cessation of flow in LCP's.[16-20] These textures usually are in the micrometer range and are interpreted in terms of spatial variations of the director axis all through the sample. The main difference between the description in terms of polydomain structure (at rest) and the textures observed under shear is that the distribution of nematic directors is in the former case constant over all the directions of space, whereas for the latter case it is anisotropic and maximum in the direction of flow. It has been suggested recently[13,21] that the textures in polymeric nematics are related to the director tumbling effects. The tumbling describes a situation in which, when subjected to a simple shear flow, the nematic director can find no preferred orientation and thus it is assumed to rotate indefinitely in the shear field.[22]

Marrucci[23] was the first to propose that these textures arise from the competition between the viscoelastic and the elastic Frank stresses. These latter ones are due to the orientational inhomogeneities of the director occurring at the transitions or walls from a domain to the next one. The Frank energy density is of the form $E_{\text{Frank}} \sim K/a^2$ where $K$ denotes some elastic constant of the material and $a$ is the average texture length scale. When compared to the viscous energy density, an expression of $a$ can be derived for the steady state regime:[23]

$$a \sim (K/\eta\dot{\gamma})^{1/2} \quad (1)$$

Here $\eta$ is its characteristic viscosity and $\dot{\gamma}$ is the shear rate at which the sample is sheared. Later on, Larson and Doi improved this phenomenological approach. Inspired by the Leslie–Ericksen theory for nematics, these authors provided a mesoscopic domain theory which, in a rather complicated way, however, relates the order parameter of the nematic state spatially averaged over domains, the total shear stress $\sigma = \eta\dot{\gamma}$, and the texture length $a$. Furthermore this model was successfully tested against rheological experiments, explaining notably the scaling laws observed in transient shear flow and strain recovery measurements.[21] The most noticeable findings of both theoretical attempts emphasize the crucial role played by the textures in the rheology of LCP's and also emphasize that the flow properties of such systems are entirely controlled through their history.[12-14]

We give here a first account of a comprehensive investigation on nematic living polymers. One basic question we wanted first to address deals with the eventual similarities of flow behaviors between the two types of liquid crystalline phases discussed above. To do so, we focus more specifically on (*i*) microscopic observations under crossed polarizers of a nematic solution during and after cessation of flow and (*ii*) the evolution of the spatially averaged order parameter of the nematic state determined from small-angle neutron scattering (SANS) spectra obtained under shear. In this report we demonstrate that the so-called band textures characteristic for LCP's also show up in nematic living polymers after cessation of the shear. The time evolution of the average band size could be determined and compared to recent theoretical predictions;[20,21] e.g. in the low shear regime the squared band spacing $a(t)$ scales linearly with the time. Finally, above a characteristic shear rate $\dot{\gamma}_c$, the nematic living polymers form an orientational monodomain which in addition is remarkably stable.

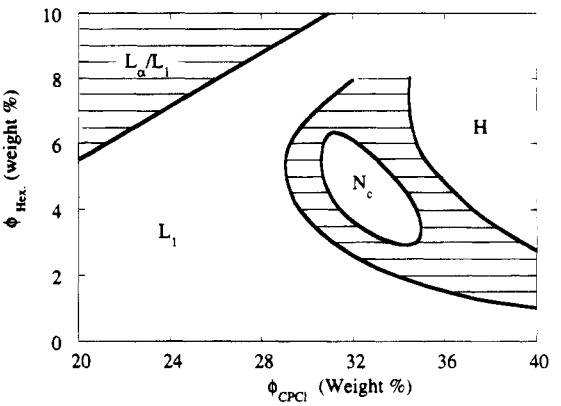


**Figure 1.** Region of the cetylpyridinium/hexanol/0.2 M NaCl-brine phase diagram showing the structural sequence, isotropic ($L_1$)/nematic calamitic ($N_c$)/hexagonal (H), related to the orientational micellar arrangement. For concentrations $\phi_{Hex} \approx 4\%$ and $\phi_{CPCl} \approx 32\%$, a nematic "island" is observed. $L_\alpha/L_1$ denotes a biphasic region where the lamellar (smectic) and disordered micellar phases coexist (hatched area). The limits are only indicative. CPCl and Hex concentrations are given in weight percent.

## II. Experimental Details and Results

**Phase Diagram and Experimental Details.** The surfactant system placed under scrutiny is the ternary solutions made of cetylpyridinium/hexanol/0.2 M NaCl-brine (hereafter abbreviated as CPCl/Hex). The structural sequence evoked in the introductory section, namely isotropic/nematic/hexagonal ($L_1/N_c/H$), observed with increasing concentration is well illustrated by the phase diagram of Figure 1 ($T = 30$ °C). For concentrations $\phi_{Hex} \approx 4\%$ and $\phi_{CPCl} \approx 32\%$, a nematic "island" is observed. Samples with different concentrations within this island have been investigated and were found to behave identically in experiments probing the dynamics or the structure of the nematic phase.

The observations of the textures during and after cessation of shear were performed at ambient temperature with the rheo-optical device described in ref 24. The shearing cell was a transparent cone (with an angle of 0.04 rad) and a transparent plate, the gap between both tools being 42 $\mu$m. The incident light was incoming perpendicular to the cone and the plate and parallel to their rotation axis, i.e. parallel to the gradient direction of the shear flow. The textures of nematic living polymers were observed using an optical polarizing microscope (with a magnification of 10) and recorded as videotapes.

The SANS measurements were performed at the Orphée Reactor at the Laboratoire Léon Brillouin on CPCl/Hex/$D_2O$ (0.2 M NaCl) solutions, which show a phase diagram similar to that of Figure 1, as far as the molar ratio [Hex]/[CPCl] is conserved.[11] A 1 mm gap Couette cell, specially designed for SANS experiments[25] was utilized as the shearing device in the range 0.1–250 $s^{-1}$. The incoming neutron beam, which encountered the sample normal to the axis of rotation of the Couette cell, was parallel with respect to the shear

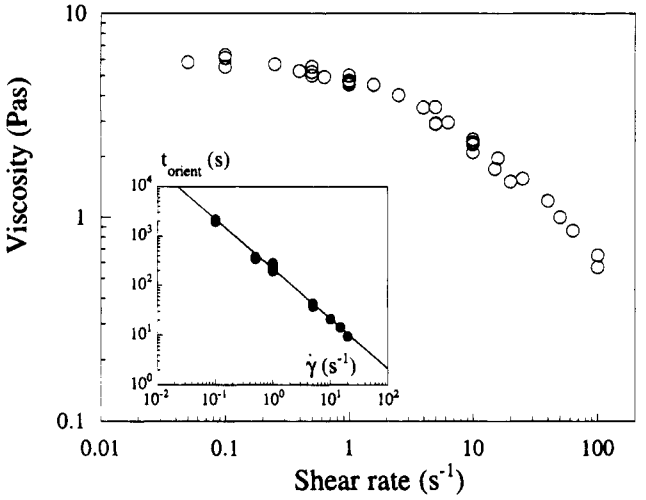


**Figure 2.** Variation of the steady state viscosity $\eta = \sigma_e/\dot{\gamma}$ as function of the shear rate for a solution of CPCl/Hex nematic living polymers with total surfactant concentration $\phi = 37\%$. Insert: $t_{orient}$, the time required for the shear stress to reach its steady state value $\sigma_e$ is plotted against the shear rate. The straight line with a slope $-1$ through the data points indicates that a constant strain is needed ($\gamma_{orient} = 220$) to reach this steady state, independent of the shear rate applied.

gradient and perpendicular with respect to the flow. This configuration was thus similar to that of the rheo-optical observations. Data were collected on a two-dimensional detector (128 × 128 elements of 0.5 × 0.5 cm$^2$) located at 2 m with a neutron wavelength $\lambda = 6.29$ Å. Shearing above a few hundred inverse seconds was prohibited due to flow instabilities at the air/solution interface.

We also present results on the viscoelastic response of the nematic CPCl/Hex solutions to a steady shear ($\dot{\gamma} = 0.05-100$ s$^{-1}$). Measurements were carried out on a Rheometrics fluid spectrometer (RFS II) working in a cone-and-plate configuration with controlled shear rate ($T = 25$ °C). At very low gradients, the transient regime could last up to 1 h, and thus an anti-evaporation device was specially constructed for the measuring cell.

**Rheology.** Since the history of a liquid crystalline solution is crucial for its rheological and structural properties, a very accurate determination of the flow behavior of the present system was achieved. Figure 2 displays the $\dot{\gamma}$ dependence of the steady viscosity for a 36% CPCl/Hex solution. The data points were obtained according to the following procedure: the sample was presheared at a fixed rate ($\dot{\gamma}_{presh} = 1$ s$^{-1}$) until the steady state conditions were reached, and then the shear rate was switched to the desired value ($\dot{\gamma} = 0.05-100$ s$^{-1}$). It was maintained until $\sigma(t)$ stabilized at its equilibrium value $\sigma_e$. The steady viscosity shown in Figure 2 was calculated from this equilibrium value of the stress. Up to ~1 s$^{-1}$, $\eta(\dot{\gamma})$ exhibits a plateau around 5.5 Pa s, followed by a shear thinning regime.

It should be emphasized that the $\sigma(t)$ profiles recorded as a function of time in a constant shear rate experiment all exhibit a transient regime characterized by damped oscillations of the stress. The overall behavior of the oscillating shear stress resembles strongly that observed in LCP's.[12-15] It is however out of the scope of the present report to discuss in detail the transient regime.[26] The time required to induce the orientation of the nematic solution $t_{orient}$ has been plotted as function of the shear rate in the insert of Figure 2. It was determined from the transient response as the time for which $(\sigma(t) - \sigma_e)/\sigma_e < 2\%$. As indicated by the straight line through the data points, one gets $t_{orient} = 220/\dot{\gamma}$. This simple power law variation means that a constant strain ($\gamma_{orient} = 220 \pm 20$) is needed to reach the steady state of shear flow in CPCl/Hex nematic solutions, or in other words that 220 strain units are necessary for such a solution to forget its own shear history. These data were essential in order to perform rheo-optical and SANS experiments under controlled shearing conditions.

**Optical Microscopy under Shear.** In the following, we focus essentially on the appearance of band textures after cessation of the flow. The nematic solution was first loaded between the transparent cone and plate. As already observed on LCP's,[20] and illustrated in Figure 3a, the sample loading induces an average orientation in the direction of the vorticity, i.e. perpendicular to both shearing and gradient directions. The width of the field of view in Figure 3a and in the following figures is 520 ± 20 μm. (Figure 3 has been reduced to 44% for publication.)

The sample was then sheared at a constant rate $\dot{\gamma}$, $\dot{\gamma}$ varying from 0.5 to 100 s$^{-1}$, for a time $t$ much longer than that defined as the orientation time $t_{orient}$ in the preceding section. Let us first briefly examine the case of the steady state of shearing ($\gamma(t) \gg \gamma_{orient}$). At low shear rates, a striped texture can be identified, with stripes parallel to the flow. The texture lengths are estimated on the order of 5−10 μm, depending on the rate applied. Moreover, we do observe a refinement of the stripes as the shear rate increases, e.g. between 0.1 and 0.5 s$^{-1}$. With a magnification of 10 as used in our rheo-optical experiments, the $a(\dot{\gamma})$ dependence could not be studied quantitatively and compared to the predictions of eq 1.

We turn now to the rheo-optical observations of textures after cessation of the shearing field. For these experiments, the samples were always prepared under identical conditions: the transparent cone was stopped after the solution had been sheared for more than 220 strain units (see previous section and Figure 2). Figures 3b and 3c show examples of band textures developing after the cessation of the flow in the direction perpendicular to it. After a preshear at 5 s$^{-1}$ the pictures were shot under a crossed polarizer and analyzer at the early (Figure 3b) and the late (Figure 3c) stages of the growth. Without polarized incoming light, these textures are no longer detectable, indicating clearly that they are due to spatial inhomogeneities of the nematic director, only. From Figure 3b and 3c, the average band spacing $a$ can be estimated at 17 and 75 μm, respectively. $a$ was estimated from the total number of bands (ranging between ~50 and 5 typically) directly counted on the video monitor. At least qualitatively, the textures in Figure 3b and 3c look very similar to those evidenced on LCP solutions.[16-20] Actually, the band textures show up at all rates between 0.5 and $\dot{\gamma}_c = 50$ s$^{-1}$ and exhibit an overall similar behavior: as time evolves, the bands broaden noticeably, with a band spacing ranging from a few micrometers to 100 μm. The textures remain stable and rather unchanged then for the next hour, until the bands transform eventually into a multidomain structure.

Concerning the time variation of the texture patterns discussed above, three preshearing rate domains can be distinguished.

I. $\dot{\gamma}_{presh} < 5$ s$^{-1}$: After an incubation time (e.g. 50 s at 0.5 s$^{-1}$ and 14 s at 1 s$^{-1}$), the bands show up and the band spacing increases regularly upon time. Actually, this incubation time has been found to vary roughly as

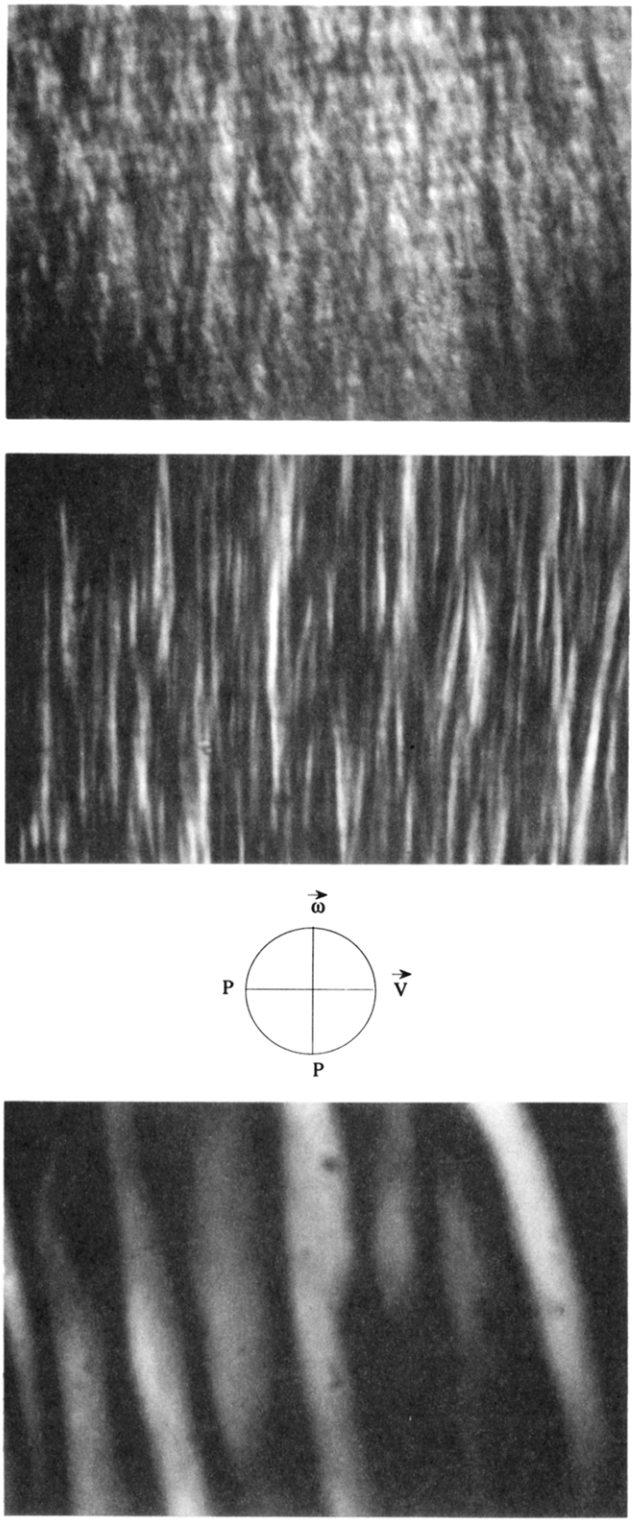


**Figure 3.** Sample of CPCl/Hex nematic solution ($\phi = 37\%$) as observed between crossed polarizers (P) using an optical polarizing microscope. The magnification is 10 and the width of the field of view 520 $\mu$m (figure reduced to 44% for publication). The solution is between the cone and the plate elements of a shearing cell working at a gap of 42 $\mu$m.[24] (a, top) After sample loading. (b, middle) After cessation of the shearing flow ($\dot{\gamma}_{presh} = 5\ s^{-1}$) at the early stage of the growth of the textures. (c, bottom) Same as (b) but at the late stage of the growth. The flow direction is shown by the vector $\vec{v}$, and $\vec{\omega}$ is the vorticity.

$\dot{\gamma}_{presh}^{-2}$ in this preshearing range. The late stage regime is characterized by a constant band spacing, typical values being 100 $\mu$m.

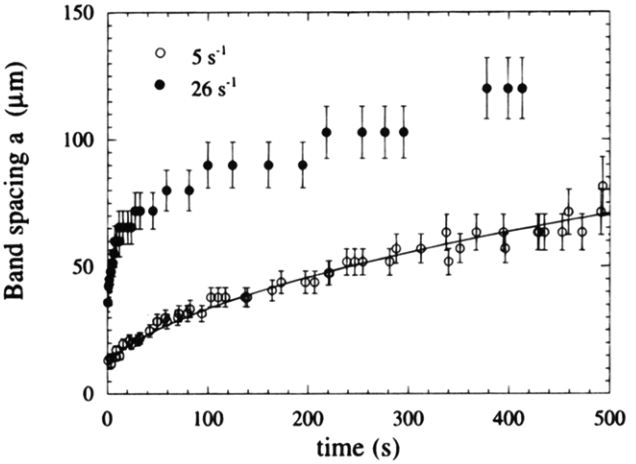


**Figure 4.** Time dependence of the average band spacing $a$ of the textures developing after cessation of the shear flow in CPCl/Hex nematic solutions. The two sets of data obtained for preshearing rates 5 $s^{-1}$ (open circles) and 26 $s^{-1}$ (closed circles) illustrate the typical behaviors for domains I and II (see text). For both shear rates, the incubation times are lower than 1 s. The continuous line results from best fit calculations using eq 3.

II. For 5 $s^{-1} < \dot{\gamma}_{presh} < 50\ s^{-1}$, no measurable incubation time could be detected. After the shear stops, the band texture appears almost instantaneously. In such cases, the band spacing increases strongly at the early stage of the growth, and then saturates at values comparable to those of the previous regime (domain I). The time dependence of the band spacing in living nematic polymer is displayed in Figure 4 for preshearing rates $\dot{\gamma}_{presh} = 5$ and 26 $s^{-1}$, illustrating the characteristic time behavior of domains I and II. The continuous line through the 5 $s^{-1}$ data points is explained in the next section.

III. $\dot{\gamma}_{presh} > 50\ s^{-1}$: No band texture could be evidenced in these cases. The solution remains homogeneously birefringent all through the measuring cell. These data suggest that the shearing has created a homogeneous monocrystalline orientation through the entire sample volume, without apparent defects. This monodomain is in addition rather stable over a long period of time. This result is corroborated using SANS under shear, as shown below.

**Small-Angle Neutron Scattering under Shear.** In Figure 5a and 5b are displayed typical two-dimensional scattering patterns for a 35.2% CPCl/Hex solution (in deuterated water) under shear. The flow direction is indicated by the arrow and the neutron beam is incoming parallel to the velocity gradient axis (i.e. perpendicular to the plane of the figures). Shear rates are 0.75 and 250 $s^{-1}$, respectively. Again, as for the rheo-optical observations, the neutron data were collected from samples which had been presheared in both cases for more than 220 strain units, so that the spectra in Figure 5 are the static structure factors of solutions in the steady state of shearing. The neutron intensities exhibit two crescent-like peaks in the direction perpendicular to the flow (shown by an arrow in Figure 5a). Such an anisotropic scattering in the form of equatorial arcs is characteristic for nematic mesophases.[9,27] It reflects the short-range translational order with respect to the center-of-mass of the micellar aggregates and the long-range orientational order driven by the flow. The sharp maximum in the $Q_\perp$ direction is at transfer momentum $Q_m = 0.11$ Å$^{-1}$, corresponding to an average distance between polymer chains of about ~60 Å. In

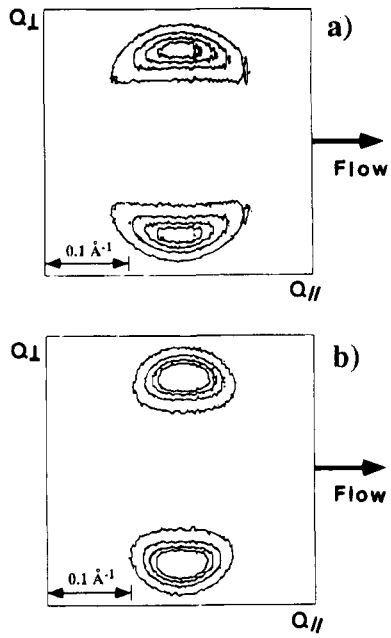


**Figure 5.** Map of elastically scattered neutron intensity obtained in SANS experiments for the nematic micellar solution of CPCl/Hex/$D_2O$ ($\phi$ = 35.2%) under shear: (a) $\dot{\gamma}$ = 0.75 $s^{-1}$; (b) $\dot{\gamma}$ = 250 $s^{-1}$. The arrow indicates the direction of flow. The SANS data were obtained at a neutron wavelength $\lambda$ = 6.29 Å on a two-dimensional detector (using 128 × 128 elements) located at 2 m from the shearing device. The contour intensities are 600, 1200, 1800, and 2400 for both spectra (arbitrary units).

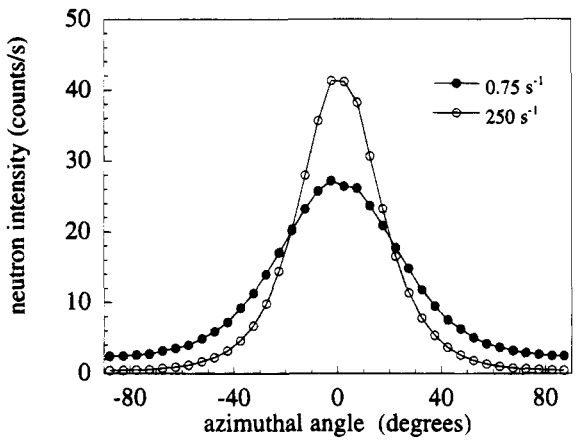


**Figure 6.** Variation of the radially integrated neutron intensity as function of the azimuthal angle $\psi$ for the $\phi$ = 35.2% CPCl/Hex solutions submitted to shear. Both intensities refer to the same 2D spectra shown in Figure 5. This neutron intensity $I(\psi)$ is then utilized in eq 4 to compute the spatially averaged order parameter $\bar{P}_2$ of the nematic phase under shear. The data shown here for $\dot{\gamma}$ = 0.75 $s^{-1}$ and $\dot{\gamma}$ = 250 $s^{-1}$ correspond to $\bar{P}_2$ values of 0.47 and 0.71, respectively.

addition, the width of the crescents in the $Q_{||}$ direction is directly connected to the distribution function of the nematic director with respect to the flow, and hence to the orientational order parameter $\bar{P}_2$.

When passing from 0.75 (Figure 5a) to 250 $s^{-1}$ (Figure 5b), this width decreases noticeably. The effect is still better evidenced in Figure 6 where, for the two spectra reported above, the data are analyzed in terms of the angular distribution of the scattered intensity. At constant azimuthal angle $\psi$, the neutron counts were integrated on momentum transfer around the maximum scattering (at $Q_m$) on a width $\Delta Q$ = ±0.02 $Å^{-1}$ and plotted *versus* $\psi$. $\Delta Q$ was taken to correspond typically to the half-width at half of the maximum scattering in the ⊥ direction.

The neutron measurements could be performed only under shear **and** in the steady state. Time-resolved experiments for instance on the transient regime of shearing or on the dynamics of the band textures were not carried out. The reason is that acceptable signal-to-noise ratios for the structure factor of these concentrated solutions are achieved with measuring times of about ~10 min. This is indeed much longer than the time required for the band textures to evolve after cessation of flow (see Figure 4). Therefore, the texture relaxations were not investigated by means of neutron scattering. However, the high $\dot{\gamma}$ range (domain III, $\dot{\gamma}_{presh}$ > 50 $s^{-1}$) characterized by the absence of band texture on the micrometer scale, has been tested with respect to neutron scattering. A nematic living polymer solution at $\phi$ = 35.2% was first presheared at 65 $s^{-1}$ well into the steady state regime ($\gamma(t) \gg \gamma_{orient}$). Neutron spectra were recorded under shear and at rest after cessation of the shear flow each ~8 min over a total time of 2 h. Surprisingly, after cessation of the flow, the neutron spectra remained unchanged within experimental accuracy, moreover, with an order parameter identical during and after the shearing period.

In order to proceed more quantitatively, the order parameter $\bar{P}_2 = \langle {}^1/_2(3\cos^2\psi - 1)\rangle$ of the nematic phase (that is, the second-order moment of the orientational distribution function) is calculated in the next section using a novel technique recently developed by Deutsch.[28]

## III. Analysis and Discussion

When subjected to a steady shear, the nematic phase of wormlike micelles behaves very similarly to liquid crystalline polymers. It should be kept in mind that the elementary objects in these phases are large cylindrical aggregates of amphiphilic molecules with lateral dimensions of 40 Å. After a transient regime estimated at $\gamma_{orient}$ = 220 units of strain (independent of $\dot{\gamma}$), the shear stress reaches its equilibrium value at $\sigma_e$. $\sigma(t)$ profiles have been found to resemble closely those obtained by Moldenaers *et al.*[12] on poly(benzyl glutamate) solutions (a complete report of this regime can be found in ref 26). As a first attempt to understand the complex flow behavior of these liquid crystalline phases, it is probably more enlightening to emphasize some crucial properties, such as the time dependence of the band textures and the orientational ordering driven by strong shearing fields. A comparison with LCP's will be also made.

**Time Dependence of the Band Texture.** As revealed by the rheo-optical measurements, striped textured develop during the shearing, with an anisotropy oriented in the direction of flow. After cessation of shear, band textures, now perpendicular to flow direction are clearly identified under crossed polarizers. As for LCP's, a so-called incubation time is needed for them to appear. This incubation time is found to vary as $\sim\dot{\gamma}_{presh}^2$, a dependence which is much stronger than that reported for LCP's (see e.g. ref 19). In addition, the time variation of the average band spacing $a$ could be determined. As illustrated in Figure 4, $a(t)$ increases with time at all preshearing rates below 50 $s^{-1}$. It should be noted that similar qualitative $a(t)$ variations were also obtained using an image analysis of the shear-induced textures on PBLG polymeric solutions.[19]

A theory however exists, which provides some clear predictions for textured materials.[21] As emphasized in

the Introduction, Larson and Doi proposed recently a mesoscopic domain theory based on the scaling arguments of Marrucci.[23] Dimensional reasoning led these authors to postulate a differential equation for the time and shear rate evolutions of the textures:

$$\frac{dL}{dt} = \alpha\dot{\gamma}L - \beta\frac{K}{\eta}L^2 \quad (2)$$

Here, $L \equiv 1/a^2$ is the total length of defect (or disclination) lines per unit volume for a nematic sample sheared at $\dot{\gamma}$ and characterized by the Frank elastic constant $K$ and the viscosity $\eta$ ($\alpha$ and $\beta$ are dimensionless constants). Two asymptotic behaviors of eq 2 are of interest for the present analysis. (*i*) The steady state shearing yields a $\dot{\gamma}^{-1/2}$ dependence of the texture length scale (as already pointed out in eq 1). (*ii*) After cessation of flow (i.e. $\dot{\gamma} = 0$ in eq 2), the texture is expected to coarsen according to

$$a^2(t) - a_0^2 = \beta\frac{K}{\eta}t \quad (3)$$

where $a_0$ denotes the mean texture size at time $t = 0$. Equation 3 has been tested against the band spacing data obtained for the CPCl/Hex nematic phase of Figure 4. In the low shear rate range (domain I, $\dot{\gamma}_{presh} < 5\ s^{-1}$), eq 3 was found to be appropriate and to account well for the 5 $s^{-1}$ data. Actually, the band spacings $a$ for preshearing rates $\dot{\gamma}_{presh} = 0.5$, 1, and 5 $s^{-1}$ are found to be superimposed on each other, and thus to obey eq 3 (only the incubation times are different between these three measurements). The full line in Figure 4 results from best fit calculations using $a_0 = 12\ \mu m$ and $\beta K/\eta = (1 \pm 0.1) \times 10^{-11}\ m^2\ s^{-1}$. Taking $\beta = 1$[23] and $\eta = 5$ Pa s (see Figure 2), one gets for the Frank elastic constant $K = 5 \times 10^{-11}$ N, a value comparable to that of LCP's.[20] At a higher shear rate (in the domain II), however, eq 3 fails to describe the $a(t)$ evolution. At the early stages of the growth, $a$ varies much faster than eq 3. This result is not surprising since, as suggested by Larson and Doi, eq 3 should be valid for simple shearing flow in the Newtonian regime only (i.e. $\sigma^e \propto \dot{\gamma}$; see Figure 2). In analogy to LCP's, we interpret the occurrence of band textures in the nematic living polymers after cessation of the shearing as resulting from a relaxation mechanism most probably associated with the defects produced by the flow.

**Orientational Monodomain at High Shear Rate ($\dot{\gamma}_{presh} > 50\ s^{-1}$, Domain III).** In order to proceed more quantitatively in the interpretation of the SANS spectra, the order parameter $\bar{P}_2$ averaged over the textures in the nematic phase has been determined from the intensity distribution $I(\psi)$ according to a novel technique developed by Deutsch.[28] Deutsch was able to derive analytic expressions relating, e.g., the second- and fourth-order parameters, the average tilt angle to the intensity $I(\psi)$ measured experimentally using neutron or X-ray scattering.

As provided in ref 28, $\bar{P}_2$ reads

$$\bar{P}_2 = 1 - \frac{3}{2N}\int_0^{\pi/2} I(\psi)\left\{\sin^2\psi + \sin\psi\cos^2\psi \times \ln\left[\frac{1+\sin\psi}{\cos\psi}\right]\right\} d\psi \quad (4)$$

Here, $N = \int_0^{\pi/2} I(\psi)\, d\psi$ is a normalizing constant. It should be emphasized that eq 4 was initially derived for a uniaxial distribution of molecules about the nematic director, *i.e.* for untextured materials. However, as already mentioned, the mesoscopic textures seem to be absent from solutions sheared above the critical shear rate $\dot{\gamma}_c = 50\ s^{-1}$, and consequently, eq 4 is appropriate to describe the state of nematic orientation in this range. In order to keep a consistent picture for the whole range in shear rates, we simply assume eq 4 to be valid below $\dot{\gamma}_c$.[29] The order parameter $\bar{P}_2$ was thus systematically calculated according to eq 4 as a function of shear rate $\dot{\gamma}$ for the three different nematic samples at $\phi = 35.2\%$ (only the hexanol concentration was allowed to change, from 3.5 to 5.2%). In Figure 7 where $\bar{P}_2$ is plotted *versus* $\dot{\gamma}$, an overall behavior is obtained. At lower shear rate (e.g. Figure 5a), the textured nematic is characterized by $\bar{P}_2$ values ~0.45–0.5 As shearing slightly increases, $\bar{P}_2$ increases noticeably and saturates around ~0.7 for $\dot{\gamma} > 50\ s^{-1}$. Although plotted differently, the behavior displayed in Figure 7 resembles strongly that of the steady-state birefringence obtained by Hongladarom *et al.* on PBLG solutions at 13% and 20%.[30] Above a transition rate, for these LCP solutions, a $\dot{\gamma}$-independent plateau of the birefringence is observed, which corresponds roughly to 90% of the monodomain value.[30]

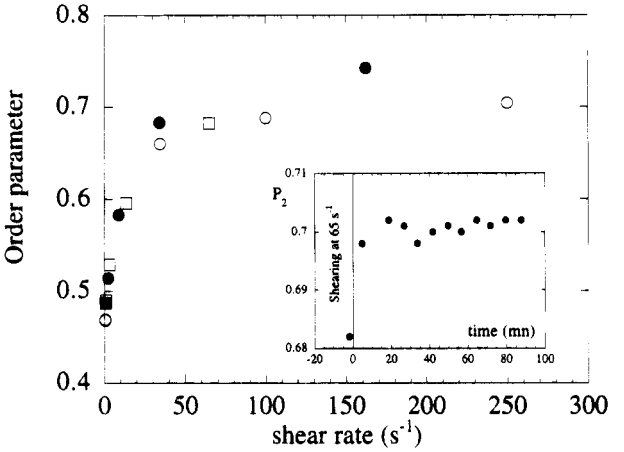


**Figure 7.** Variation of the order parameter $\bar{P}_2$ of nematic phases of CPCl/Hex wormlike micelles as calculated from 2D-SANS spectra. The different labels denote different hexanol concentrations, the total surfactant concentration $\phi$ remaining identical, $\phi = 35.2\%$: $\phi_{Hex} = 3.5\%$ (squares), 4.3% (open circles), and 5.3% (closed circles). Above the critical shear rate, $\dot{\gamma}_c = 50\ s^{-1}$, $\bar{P}_2$ saturates around ~0.7. Insert: time evolution of the order parameter for a nematic sample having been presheared at 65 $s^{-1}$.

The insert of Figure 7 exhibits the time evolution of the order parameter $\bar{P}_2$ in the experiments described in the previous section. After being presheared at 65 $s^{-1}$, neutron spectra were recorded each ~8 min over 2 h. As a result, $\bar{P}_2$ is found to be constant at 0.7 during and after the shearing period. This is not the case when similar experiments are carried out in domains I and II (here, the spectra in the steady state and at rest are noticeably different). Note that the slight increase at $t = 0$ (at which the Couette cell has been stopped) is less than the uncertainty in the $\bar{P}_2$ determination (±2%). Confirming the absence of texture relaxations seen by optical microscopy in this $\dot{\gamma}$ range (domain III), this result suggests that once sheared above $\dot{\gamma}_c = 50\ s^{-1}$, the nematic solution forms an orientational monodomain. This monodomain, moreover, seems to be remarkably stable.

The neutron data deserve additional comments. In the experimental configuration of the PAXY instrument at the Laboratoire Léon Brillouin, the neutrons ($\lambda = 6.29$ Å) provide information on the nematic arrangement of

the polymer-like chains on a 100 Å scale. However, the intensity received on the detector is the response averaged over a scale which is much larger, typically given by the section of the incoming neutron beam (0.5 $cm^2$). It is thus integrated over the textures seen by optical microscopy at rest or under shear. Therefore, in the steady state, at least three contributions have to be considered for the orientational distribution function experienced by neutron scattering. In other words, in a steady shear experiment at low gradient ($\dot{\gamma} = 1\ s^{-1}$), the broadening of the crescent-like peaks along the equatorial arcs (Figure 6) is due to (*i*) the thermal fluctuations of the polymer chains within an oriented domain with a given director, (*ii*) the distribution of director orientations of the domains in the striped texture regime, and (*iii*) defects or disclinations produced by the flow. The first contribution can be related to the order parameter of a uniformly oriented monodomain, whereas the second one refers to a mesoscopic order parameter associated with the polydomain textures. In the present neutron experiments at low shear rate, $\dot{\gamma} < 50\ s^{-1}$, it is clear that we cannot identify any of these three contributions separately. This is not the case for domain III of shearing where both rheo-optical and neutron data suggest that no texture relaxation occurs after cessation of the flow. Here, the $\bar{P}_2$ data received from eq 4 ($\bar{P}_2 \sim 0.7$) can be interpreted as arising from an orientational monodomain of wormlike micelles. It can then be assumed that the thermal fluctuations related to the micellar flexibility are then only contributing to the order parameter of the nematic phase.

## IV. Concluding Remarks

Combining viscoelastic, rheo-optical measurements, and small-angle neutron scattering under shear on nematic solutions of living polymers, we have shown that the orientation and texture properties of these systems bear strong similarities to those of liquid crystalline polymers.

As remarkable features, there are the following.

(a) In a simple shear experiment, the steady state is obtained for a given deformation $\gamma_{orient} = 220 \pm 20$, independent of the shear gradient applied. In other words, this means that 220 strain units are necessary for a solution of nematic living polymers to forget its own shear history.

(b) After cessation of the flow, band textures appear perpendicular to the flow direction, indicating a modulation of the director orientation. As for LCP's, these textures are interpreted in terms of relaxation of the Frank distorsional energy accumulated during the flow.

(c) With increasing shear rates, the order parameter $\bar{P}_2$ of the nematic phase (determined from bidimensional neutron spectra) increases from 0.45 at low gradients and then saturates at 0.7 above $50\ s^{-1}$. This approach in terms of order parameter demonstrates that wormlike micelles in their nematic state are easily aligned with respect to the flow.

Two additional features have been discussed in detail, the time dependence of the band texture after cessation of flow and the existence of an orientational and stable monodomain for solutions sheared above a critical rate, $\dot{\gamma}_c = 50\ s^{-1}$. For the former point, moreover, we demonstrate that the time evolution of the band spacing $a$ is in agreement with recent theoretical predictions made by Larson and Doi for textured materials, i.e. $a^2(t) \sim t$. For the later point, however, there remains an open question. According to eq 1, the average size of the domains in the steady state *decreases* with increasing $\dot{\gamma}$ (as $a \sim \dot{\gamma}^{-1/2}$). Such an expectation seems to disagree with the existence of an orientational monodomain (which can be seen as a divergence of $a$) induced by strong shearing, as revealed by rheo-optical and SANS experiments. In order to have more insight on the complex flow and orientation behaviors of the nematic living polymers, time-resolved X-ray and neutron scattering experiments should be very helpful.

**Acknowledgment.** We would like to thank M. Brunet, P. Navard, and G. Marrucci for helpful discussions and comments. M. Brunet is also acknowledged for her support in using her video and microscopy facilities.

## References and Notes

(1) For a review: Cates, M. E.; Candau, S. J. *J. Phys. Condens. Matter* **1990**, *2*, 6869.
(2) Appell, J.; Porte, G. *Europhys. Lett.* **1990**, *12*, 185. Idem. *Prog. Colloid* Polym. *Sci.* **1991**, *84*, 41.
(3) Cates, M. E. *Macromolecules* **1987**, *20*, 2289. Idem. *J. Phys.* **1988**, *49*, 1593. Granek, R.; Cates, M. E. *J. Chem. Phys.* **1992**, *96*, 4758 and references therein.
(4) Rehage, H.; Hoffmann, H. *Mol. Phys.* **1991**, *74*, 933 and references therein.
(5) Khatory, A.; Lequeux, F.; Kern, F.; Candau, S. J. *Langmuir* **1993**, *9*, 1456.
(6) Terech, P.; Schaffhauser, V.; Maldivi, P.; Guenet, J. M. *Langmuir* **1992**, *8*, 2104.
(7) Clausen, T. M.; Vinson, P. K.; Minter, J. R.; Davis, H. T.; Talmon, Y.; Miller, W. G. *J. Phys. Chem.* **1992**, *96*, 474.
(8) Berret, J. F.; Appell, J.; Porte, G. *Langmuir* **1993**, *9*, 2851. Berret, J.-F.; Roux, D. C.; Porte, G. *J. Phys.* **1994**, *4*, 1261.
(9) Hendrikx, Y.; Charvolin, J.; Rawiso, M.; Liébert, L.; Holmes, M. C. *J. Phys. Chem.* **1983**, *87*, 3991. Using the terminology of these authors, *calamitic* refers to elementary aggregates with a cylindrical morphology, and not discotic.
(10) El Haitamy, O. Thèse de troisième cycle, Université de Montpellier France, 1985, unpublished.
(11) Berret, J.-F.; Roux, D. C.; Porte, G.; Lindner, P. *Europhys. Lett.* **1994**, *25*, 521.
(12) Moldenaers, P.; Mewis, J. *J. Rheol.* **1986**, *30*, 567. Moldenaers, P.; Yanase, H.; Mewis, J. *J. Rheol.* **1991**, *35*, 1681.
(13) Burghardt, W. R.; Fuller, G. G. *Macromolecules* **1991**, *24*, 2546.
(14) Hongladarom, K.; Burghardt, W. R. *Macromolecules* **1993**, *26*, 785.
(15) Navard, P.; Haudin, J. M. *J. Polym. Sci., Polym. Phys. Ed.* **1986**, *24*, 189.
(16) Kiss, G.; Porter, R. S. *Mol. Cryst. Liq. Cryst.* **1980**, *60*, 267.
(17) Donald, A. M.; Viney, C.; Windle, A. H. *Polymer* **1983**, *24*, 155.
(18) Navard, P.; Zachariades, A. E. *J. Polym. Sci.* **1987**, *25*, 1089. Ernst, B.; Navard, P. *Macromolecules* **1989**, *22*, 1419.
(19) Gleeson, J. T.; Larson, R. G.; Mead, D. W.; Kiss, G.; Cladis, P. E. *Liq. Cryst.* **1992**, *11*, 341.
(20) Larson, R. G.; Mead, D. W. *Liq. Cryst.* **1992**, *12*, 751.
(21) Larson, R. G.; Doi, M. *J. Rheol.* **1991**, *35*, 539.
(22) Dubois-Violette, E.; Durand, G.; Guyon, E.; Manneville, P.; Pieranski, P. *Solid State Phys. Suppl.* **1978**, *14*, 147.
(23) Marrucci, G. *Pure Appl. Chem.* **1985**, *57*, 1545.
(24) Riti, J. B.; Navard, P. *Synth. Polym.*, to be published.
(25) Lindner, P.; Oberthür, R. C. *Rev. Phys. Appl.* **1984**, *19*, 759.
(26) Berret, J.-F.; Roux, D. C., Manuscript in preparation.
(27) Murthy, N. S.; Knox, J. R.; Samulski, E. T. *J. Chem. Phys.* **1976**, *65*, 4835. Oldenburg, R.; Wen, X.; Meyer, R. B.; Caspar, D. L. D. *Phys. Rev. Lett.* **1988**, *61*, 1851. Keates, P.; Mitchell, G. R.; Disdier, E.; Navard, P. *Polymer* **1993**, *34*, 1317.
(28) Deutsch, M. *Phys. Rev. A* **1991**, *44*, 8264.
(29) Note in addition that the $\bar{P}_2$ data received from eq 4 and shown in Figure 7 are probably underestimated since the neutron intensity was not deconvoluted with respect to the experimental function of the neutron spectrometer. A more sophisticated treatment is then necessary for a quantitative analysis of the $\bar{P}_2$ values *versus* $\dot{\gamma}$.
(30) Hongladarom, K.; Burghardt, W. R.; Baek, S. G.; Cementwala, S.; Magda, J. J. *Macromolecules* **1993**, *26*, 785.

MA9412647